Section 3
ADVANCED TECHNOLOGY DEVELOPMENTS

3.A Time-Dependent Semiclassical Theory of Gain-Coupled Distributed Feedback Lasers

Recent interest in the transient behavior of distributed feedback lasers (DFL) has created the need for a more complete theoretical analysis than has existed previously. The photon rate equation model used by Zs. Bor[1] treats the time dependence of the laser output, but due to the mean field approximation inherent in this theory it is unable to treat the regime where spatial propagation and cavity length become important in determining the output pulse duration. This regime is of particular interest because of the possibility of producing single pulses of picosecond duration from such lasers.

The fundamental characteristic of a distributed feedback laser is that in the absence of external mirrors, the necessary feedback is provided by Bragg scattering from spatially periodic variations of the complex refractive index of the laser medium. This can be either the real component or the imaginary component (gain) of the material index or the effective index (as in an optical waveguide). In the case where the gain is used to vary the complex index, a nonlinear coupling occurs between the gain and the optical field. As the light intensity in the excited region increases, the gain is depleted, destroying the feedback and allowing the light to escape the medium. This self cavity-dumping can, for a range of pump energies, produce a train of ultrashort pulses. Typically these pulses are 50-100 times shorter than the pump pulse used.[2]

Semiclassical Theory of DFL

As in the rate equation theory,[1] the gain medium is modeled according to Fig. 18.21. Following the approach of Sargent *et al.*,[3] the system is described by the equations for the density matrix:

$$\dot{\rho}_{11} = -\gamma_{10}\rho_{11} + \gamma_{21}\rho_{22} + \left(\frac{i}{\hbar} V_{21}\rho_{12} + \text{c.c.}\right) \tag{1a}$$

$$\dot{\rho}_{22} = \lambda_2 - \gamma_{21}\rho_{22} - \left(\frac{i}{\hbar} V_{21}\rho_{12} + \text{c.c.}\right) \tag{1b}$$

$$\dot{\rho}_{21} = -(i\omega_o + \gamma)\,\rho_{21} + \frac{i}{\hbar} V_{21}\,(\rho_{22} - \rho_{11}). \tag{1c}$$

Note that ρ_{ii} is the population of level i, and γ is the homogeneous linewidth of the lasing transition. $V_{21} = -pE(z,t)$ is the atomic interaction energy, p is the dipole matrix element, and $E(z,t) = \frac{1}{2}[A(z,t)\exp(i\omega t) + \text{c.c.}]$ is the electric field in terms of the slowly varying envelope A(z,t). Here c.c. denotes the complex conjugate.

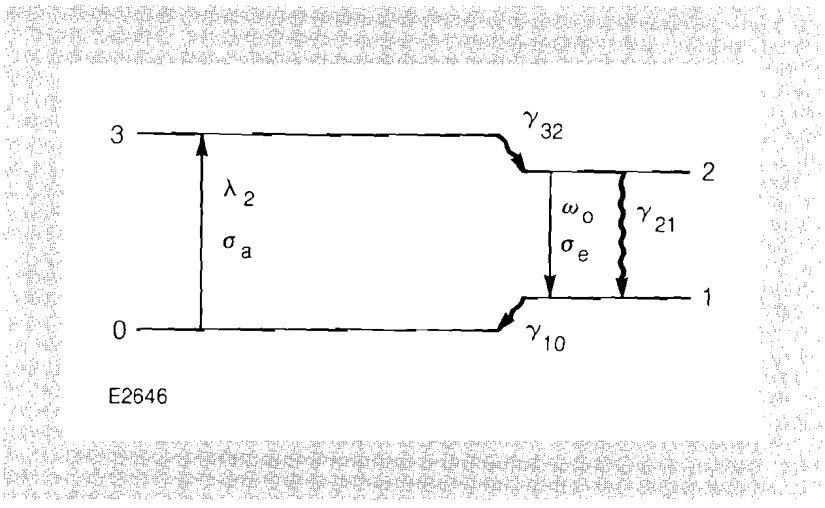

Fig. 18.21
The four-level system used for both the photon and semiclassical rate equations. The decay rates γ_{32} and γ_{10} are assumed to be large.

The density-matrix equations can be simplified by making the rate equation approximation for the gain medium (not the fields), which is valid when the linewidth γ is sufficiently large.[3,4] After formally integrating Eq. (1c) and assuming that A(z,t) and the population inversion $w(z,t) \equiv \rho_{22} - \rho_{11}$ vary little in time, γ^{-1}, ρ_{21} becomes approximately

$$\rho_{21} = \frac{-ip}{2\hbar}\,\frac{A^* w}{i\Delta + \gamma}\,e^{-i\omega t} \tag{2}$$

where $\Delta = \omega_o - \omega$ and nonresonant terms have been neglected (rotating wave approximation[5]). Substituting Eq. (2) into Eqs. (1a) and (1b) leads to

$$\dot{\rho}_{22} = \lambda_2 - \gamma_{21}\rho_{22} - \frac{p^2}{2\hbar^2}\,\frac{\gamma}{\Delta^2 + \gamma^2}\,|A|^2 w \tag{3a}$$

$$\dot{\rho}_{11} = \gamma_{21}\rho_{22} - \gamma_{10}\rho_{11} + \frac{p^2}{2\hbar^2}\,\frac{\gamma}{\Delta^2 + \gamma^2}\,|A|^2 w. \tag{3b}$$

The equations are further simplified by assuming that γ_{10} is large so that $\rho_{11} \ll \rho_{22}$ and $w \simeq \rho_{22}$. Then the inversion w obeys

$$\dot{w} = \lambda_2 - \gamma_{21}\, w - B\,|A|^2 w \tag{4}$$

where

$$B = \frac{p^2}{2\hbar}\left(\frac{\gamma}{\Delta^2 + \gamma^2}\right).$$

To provide feedback for the gain-coupled DFL the pumping rate λ_2 is spatially modulated with a period $\Lambda = \pi/\beta_0$,

$$\lambda_2 = N\lambda(t)\,(1 + V \cos 2\beta_0 z)$$

where, again, V is the visibility of the fringes and where $\lambda(t)$ accounts for the time dependence of the pumping, which may be provided by a laser pulse. To remove the rapid spatial modulation from the equations, and to go to a macroscopic description, a new inversion density variable W is defined by

$$W = \frac{Nw}{1 + V \cos 2\beta_0 z}\,. \tag{5}$$

The equation for the time dependence of W is then, from Eq. (4),

$$\dot{W} = N\lambda - \gamma_{21}\, W - B\,|A|^2 W. \tag{6}$$

The field evolution is determined by the wave equation,

$$\left[\frac{\delta^2}{\delta z^2} - \frac{n^2}{c^2}\,\frac{\delta^2}{\delta t^2}\right] E(z,t) = \frac{4\pi n^2}{c^2}\,\frac{\delta^2}{\delta t^2}\,P(z,t) \tag{7}$$

where the polarization $P = \frac{1}{2}\,[P(z,t) \exp(i\omega t) + c.c.]$.

If A(z,t) is separated into two counter-propagating waves

$$A(z,t) = Re^{i\beta_0 z} + Se^{-i\beta_0 z} \tag{8}$$

and substituted into Eq. (7) we obtain (ignoring second derivatives of R and S as well as the first derivative of P)

$$\left[i\beta_0 R' - \frac{1}{2}\left(\beta_0^2 - \frac{\omega^2 n^2}{c^2}\right)R - \frac{i\omega n^2}{c^2}\,\dot{R}\right] e^{+i\beta_0 z}$$

$$-\left[-\,i\beta_0 S' - \frac{1}{2}\left(\beta_0^2 - \frac{\omega^2 n^2}{c^2}\right)S + \frac{i\omega n^2}{c^2}\,\dot{S}\right] e^{-i\beta_0 z} = \frac{2\pi n^2 \omega^2}{c^2}\,P \tag{9}$$

where a prime (e.g., R′) indicates a partial derivative with respect to z. In the semiclassical theory the polarization is determined by

$$P = 2Np\,\rho_{12} e^{-i\omega_0 t}. \tag{10}$$

Using the value of $\rho_{12} = \rho_{21}^*$ from Eq. (2) we get

$$P = -\frac{iNp^2}{\hbar}\frac{Aw}{i\Delta+\gamma} . \tag{11}$$

Significant feedback occurs only for $\beta \simeq \beta_0$. Using this fact and Eq. (11), Eq. (9) can be separated into the following two equations:

$$R' - \frac{n}{c}\dot{R} + (\alpha W - i\delta)\, R = -\frac{\alpha V W}{2}\, S \tag{12a}$$

$$-S' - \frac{n}{c}\dot{S} + (\alpha W - i\delta)\, S = -\frac{\alpha V W}{2}\, R \tag{12b}$$

where $\delta = (\beta^2 - \beta_0^2)/2\beta_0$ and $\alpha = 2\pi\beta Np^2/\hbar(i\Delta+\gamma)$. Equations (12a) and (12b) were obtained by neglecting terms in $\exp(\pm i3\beta_0 z)$, i.e., by assuming that W is slowly varying spatially. This neglects spatial hole burning, which has been found to be relatively unimportant, in agreement with the steady-state case.[3]

Depletion of the ground state, level 0, is accounted for in the normal manner through the pump term $\lambda(t)$, i.e., by replacing

$$\lambda N \rightarrow \lambda(N-W). \tag{13}$$

In order to simulate spontaneous emission, a uniform noise term equivalent to one photon in the excited region was introduced into the field equations. The time-averaged energy is

$$\overline{\int_{V_0} \frac{E_0^2}{4\pi} dV} = \hbar\omega_0 .$$

where the integral is over the volume V_0 of the excited region. Assuming the noise to be equal in both directions, we find for the noise fields

$$R_0 = S_0 = \sqrt{\frac{4\pi\hbar\omega_0}{V_0}} . \tag{14}$$

The final equations are then,

$$R' - \frac{n}{c}\dot{R} + (\alpha W - i\delta)\,(R+R_0) = -\frac{\alpha W V}{2}\, S \tag{15a}$$

$$-S' - \frac{n}{c}\dot{S} + (\alpha W - i\delta)\,(S+S_0) = -\frac{\alpha W V}{2}\, R \tag{15b}$$

$$\dot{W} = \lambda(N-W) - \gamma_{21}\, W - B\,(|R|^2 + |S|^2)W. \tag{15c}$$

In going from Eq. (6) to Eq. (15c) the cross terms of $|A|^2$ were neglected, consistent with the assumption of no spatial hole burning.

DFL Calculations

Equations (15a), (15b), and (15c) were solved numerically. Due to the counter-propagating nature of the field solutions a second-order Euler method was used which required a square integration grid ($\Delta z = c\Delta t$). The equations were integrated subject to the boundary conditions that $S(L,t) = R(0,t) = W(z,0) = 0$, and that $\lambda(t)$ be Gaussian in time and uniform in space.

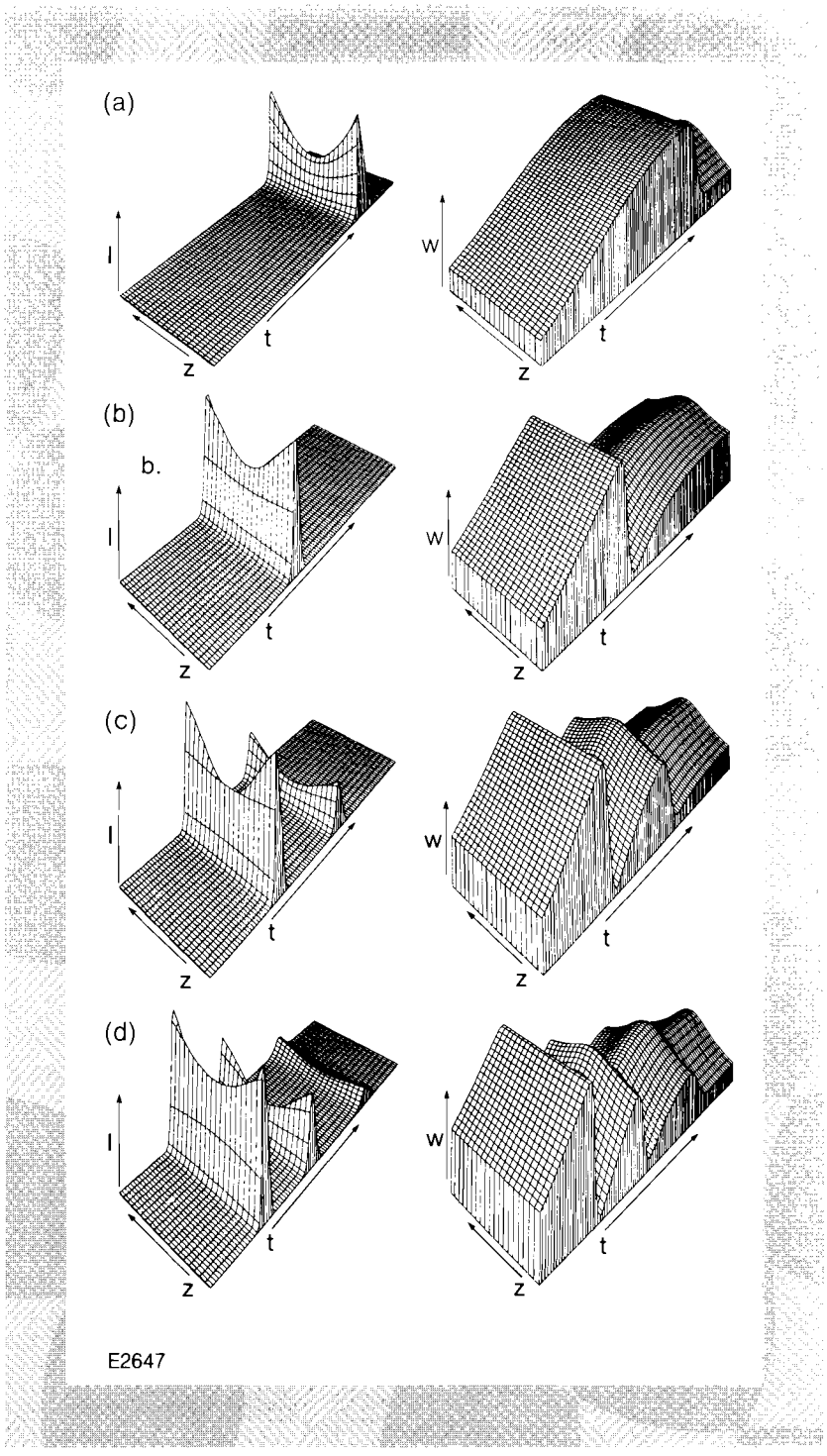

Fig. 18.22
Total intensity $I = R^2 + S^2$ and population inversion density W plotted as functions of time and space for an increasing pump energy. The pump-pulse duration was 70 ps, and the pumped region was 0.1 cm in length. The relative values of the pump energies are (a) 0.5, (b) 1.1, (c) 1.5, and (d) 2.0. The vertical scales are normalized, and the time axis represents 120-ps full scale.

The system parameters were chosen appropriate for Rhodamine 6G in ethylene glycol as the active medium in the distributed feedback laser, i.e., $N = 3.5\times10^{-3}$ M (2.1×10^{18} mol/cm^2), $V_0 = bL/N\sigma_a$, $b = 0.025$ cm, $\sigma_a = 2.7\times10^{-16}$cm^2, $\alpha = \sigma_e/2$, $\sigma_e = 1.4\times10^{-16}$cm^2, $\tau = 1/\gamma_{21} = 4$ ns, $V = 1.0$, $n = 1.44$.

Due to the nonlinear coupling between the gain, the Bragg reflectivity, and the field, a self cavity-dumping is observed for a range of pump energies in the DFL. The inversion builds up as the integral of the pump pulse until the field increases sufficiently for gain saturation to become dominant. At this time, the Bragg reflectivity decreases rapidly allowing the field to escape as a pulse. If this process occurs during the pump pulse, the inversion has the opportunity to recover and produce a second pulse. As the pump energy is increased, the initial dumping will occur at earlier times allowing additional pulses to be produced. In Fig. 18.22, the total intensity $I = R^2 + S^2$ and population inversion W are shown for a sequence of increasing pump energies. The solutions are plotted as functions of space and time. The laser output is directly proportional to the value of the total intensity at the end face ($z = 0,L$) of the pumped region. The behavior of these solutions at the end faces is in very close qualitative agreement with the photon rate equation model.[1]

Using the previously published predictions[6] of the photon rate equations for the duration of the initial output pulse as a function of the length of the pumped region given that either (a) the second pulse is at threshold or (b) the third pulse is at threshold, the new theory can be quantitatively evaluated as to its performance in the limit of long pump pulses, $T_p \gg nL/c$. This comparison is shown in Fig. 18.23 for a pump pulse of 3.5 ns. The results show excellent agreement between the two theories in this limit. It is interesting to note that, although there is an offset, the slope of the dependence is very close to that of the line $t = nL/c$.

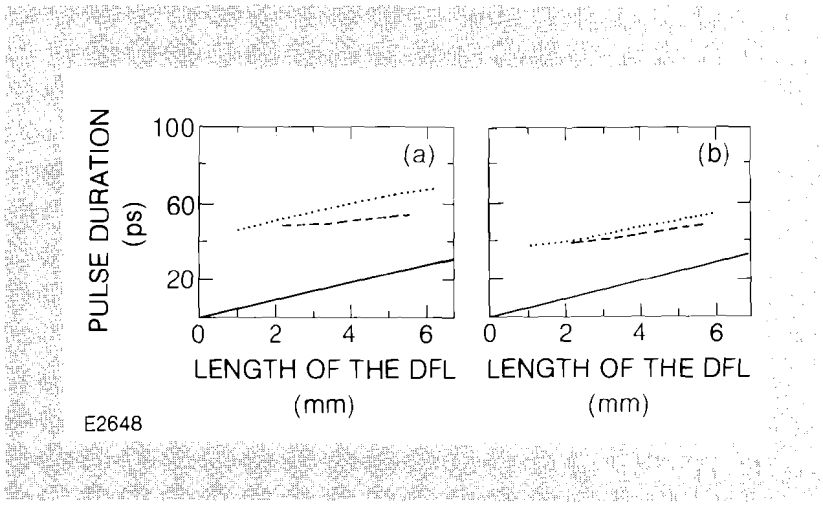

Fig. 18.23
Duration of the first pulse as a function of the length of the DFL for a 3.5-ns pump pulse and (a) the second pulse at threshold, and (b) the third pulse at threshold. The dashed line corresponds to the photon rate equation prediction, and the dotted line to the semiclassical prediction. The solid line is $t = nL/c$.

It has been shown previously that as the pump pulse width is reduced, the pulse duration of the DFL will also shorten.[2] However, as the pump pulse duration becomes comparable to the pumped-region transit time ($T_p = nL/c$) the photon rate equation analysis will be

invalid. In Fig. 18.24, the predicted pulse width versus pumped-region length [similar to Fig. 18.23(a)] in the case of a 70-ps pump pulse is shown for the two theories. Again, the line t=nL/c is shown. A large discrepancy between the theories is evident which, as expected, decreases as the length of the pumped region is decreased. It is seen that the pulse widths are much longer than predicted by the photon rate equations and that their duration approaches the transit time nL/c.

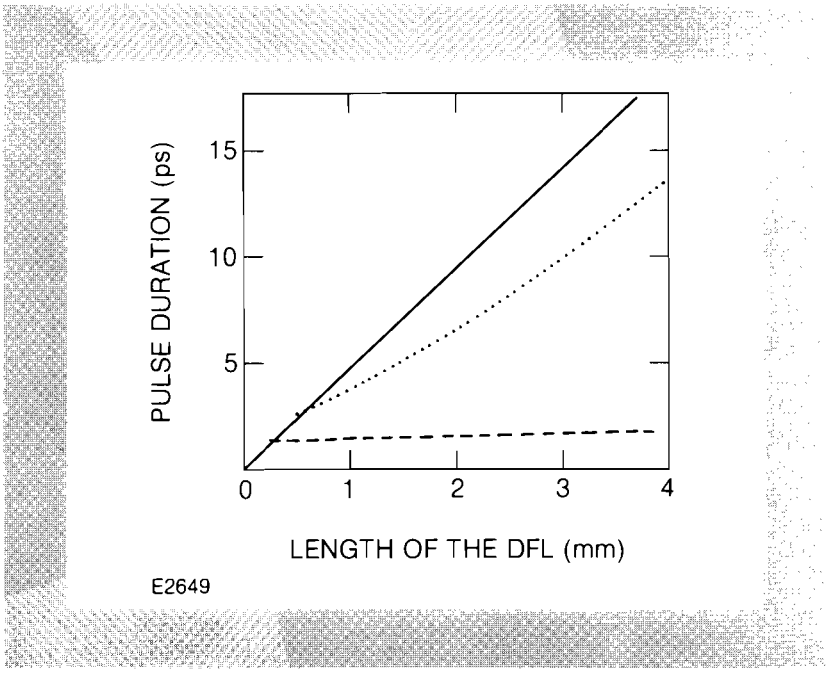

Fig. 18.24
Duration of the first pulse as a function of the length of the DFL for a 70-ps pump pulse and the second pulse at threshold. The dashed line is that predicted by the photon rate equation model, and the dotted line is that predicted by the semiclassical theory. The solid line is t = nL/c.

In the steady-state limit, $\dot{S} = \dot{R} = 0$, the field equations (12) reduce directly to the form of previous steady-state theories[3,7] in the gain-coupled case. The amount of Bragg reflectivity at any point is proportional to the coefficient of the coupling term in the field equations. The value of this coupling coefficient determines the nature of the field distribution. For a gain-coupled laser, the coupling coefficient can be expressed as αVWL/2. It has been shown in the steady-state analyses that if $\alpha VWL/2 < 1.5$, termed undercoupled, the field distribution will be peaked toward the ends of the pumped region, while if $\alpha VWL/2 > 1.5$, termed overcoupled, the distribution will be peaked in the center of the cavity. In the case of steady-state pumping shown in Fig. 18.25, after the initial oscillations damp out, the coupling coefficient can be calculated for different positions in the pumped region. The coupling coefficient varies from 0.42 at the edge of the region (z = 0,L) to 1.3 in the center (z = L/2) where it is at a maximum. This evaluation agrees with the form of the intensity distribution seen in Fig. 18.25(c), which shows behavior typical of undercoupling.

We have found that due to gain saturation in a laser of this type, the high values of αVWL required for overcoupled operation cannot be maintained in the steady state. However, during the transient field build-up, prior to gain saturation, the coupling coefficient can reach values in the overcoupled range. This results from the gain over-

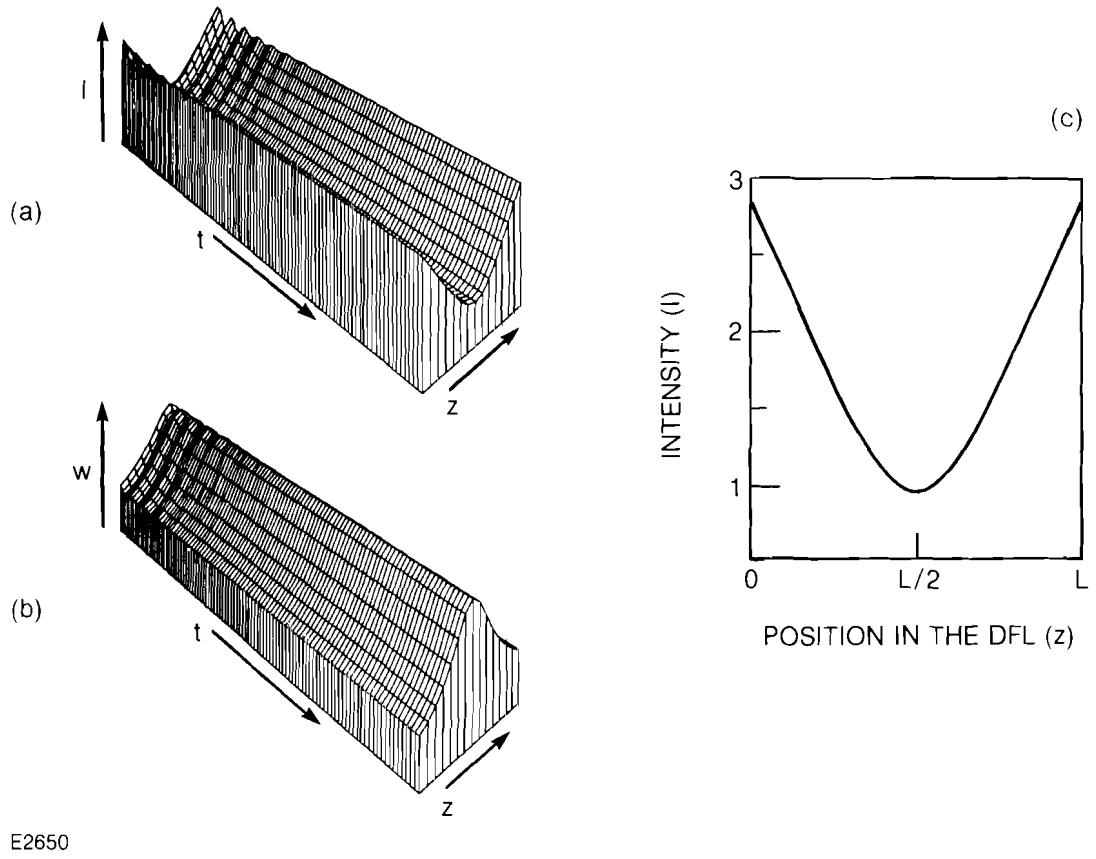

Fig. 18.25
The intensity I and inversion density W as functions of space and time for steady-state pumping (a, b) and the final intensity distribution along the length of the DFL (c). The length of the DFL was 0.3 cm.

shooting the steady-state value prior to the field build-up. As the field builds up, it experiences strong coupling and, therefore, peaks in the center of the cavity. Then, as the transient field depletes the gain, the laser shifts to the undercoupled regime enabling the pulse to escape. In Fig. 18.26, 3-D plots of two cases are shown. For each case the plot is viewed both from earlier times [Figs. 18.26(a) and 18.26(c)] , and from later times [Figs.18.26(b) and 18.26(d)] to allow examination of the intensity distribution as it evolves. In Fig. 18.26(a), the contours of equal time can be seen to have positive curvature indicating an overcoupled intensity distribution, while at later times [Fig. 18.26(b)], the contours show the negative curvature typical of undercoupled operation. Figures 18.26(c) and 18.26(d) are the same views of the field when the pumped region is made shorter. In this case the operation is undercoupled ($\alpha VWL/2 < 1.5$) even during the buildup, as seen by negative curvatures at all times.

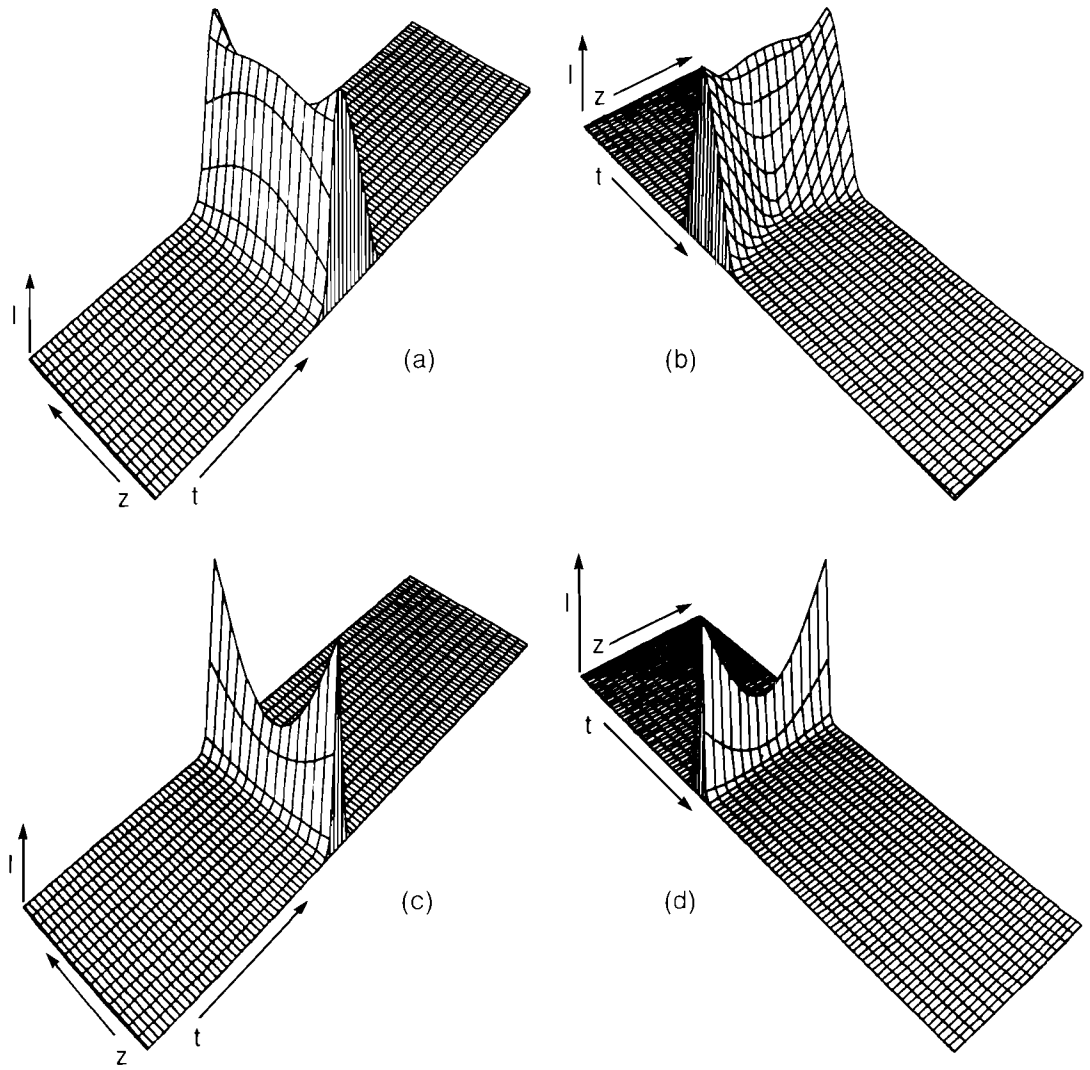

Fig. 18.26
The intensity as functions of space and time for the case of the DFL of length 0.3 cm (a, b) and 0.03 cm (c, d). In both cases the pump intensity was adjusted so that the second pulse was at threshold. For each case the intensity distribution is shown as seen from earlier times (a, c) or from later times (b, d).

Conclusion

Due to the inability of the photon rate equation analysis of the DFL to predict the output characteristics accurately in the regime where the pumped-region transit time is comparable to the pump pulse length, a semiclassical treatment has been developed which takes into account the spatial variation of the field and inversion along the pumped region. The addition of this consideration provides a theory capable of handling both the short-time transient regime and the